



The photocatalytic oxidation of dibenzothiophene (DBT)

Ronald Vargas, Oswaldo Núñez*

Laboratorio de Química Ambiental, Departamento de Procesos y Sistemas, Universidad Simón Bolívar, Sartenejas, Caracas 89000, Apartado postal 8900, Venezuela

ARTICLE INFO

Article history:

Received 10 January 2008

Received in revised form 5 August 2008

Accepted 7 August 2008

Available online 14 August 2008

Keywords:

TiO₂-UV solar light

Dibenzothiophene (DBT)

degradation-mineralization

DBT 5,5-dioxide (DBT sulfone)

Langmuir-Hinshelwood

Triton X-100

ABSTRACT

TiO₂/UV solar light degradation of dibenzothiophene (DBT) aqueous solutions readily occurs in neutral and acid media. For instance, at neutral pH, $t_{1/2} = 30$ min are found for DBT degradation and mineralization. In neutral and acid media the rate limiting step for mineralization is the same as for degradation and corresponds to the DBT sulfone formation. Benzaldehyde is the major reaction product. In addition, it also acts as an intermediate in the mineralization to CO₂ + water + sulfate. The results support the Langmuir-Hinshelwood degradation mechanism. Therefore, instead of pseudo-first-order rate constants, apparent rate constants that depend on concentration are obtained. Only at basic pH these apparent rate constant are independent of the [DBT]₀. The solubility of DBT in water is increased by one-order of magnitude when solutions of the surfactant Triton X-100 is used at [Triton X-100] > CMC (critical micelle concentration). Under these conditions DBT is readily degraded without degrading Triton X-100 at $t_{1/2}$ ca. 120 min. DBT is solubilized into Triton X-100 micelles from where it exchanges with water and becomes available for degradation. Triton X-100 monomers slightly compete with DBT for the TiO₂ catalytic site.

The degradation method established in this work might be used, for instance, to decontaminate soil contaminated with sulphur-rich heavy oil following a pre-treatment consisting of washing out the solid with Triton X-100 solutions, prior to photolysis.

© 2008 Elsevier B.V. All rights reserved.

1. Introduction

Oxidative desulfuration [1,2] has evolved as an alternative for removal of sulfur compounds [3,4] that are resistant to hydrodesulfuration or thermal extrusion. Among these compounds is dibenzothiophene (DBT) an organic sulfur derivative considered as representative of the hydrocarbons in the asphaltene fraction. Various oxidants have been used to produce ultra-low sulfur fuels. Among them, are hydroperoxides [5,6], peroxyacids [7], nitrogen oxide [8] and nitric acids [8,9]. Hydrodesulfuration followed by biodesulfuration has also been used [10] on DBT as a model compound. Studies to improve hydrodesulfuration of DBT using metal compounds such as tris(triethylphosphine)platinum (0) are also known in the literature [11]. Oxidation of DBT derivatives using 12-tungstophosphoric acid (TPA) in biphasic systems has also been reported [12]. Photocatalytic degradation of sulphur-containing aromatic compounds in the presence of zeolite-bound triphenylpyrylium compound has also been reported [13]. However, the use of an advanced oxidation method such as UV-TiO₂ on DBT is not common in literature. This is probably due to its relatively low solubility in water. However, the solubility could be increased by

using surfactant solutions. We have been working on photocatalytic degradation (in water) of different crude oil [14] fraction components, for instance, naphthalene, as a model of the polyaromatic components of the hydrocarbons. In order to improve naphthalene solubility in water, we have used the surfactant Triton X-100 (polyethylene glycol *p*-(1,1,3,3-tetramethylbutyl)-phenyl ether). In fact, we have found conditions to degrade naphthalene with Triton X-100 in solution intact [15]. We have also recently reported [16] the efficiency of the method for degrading nitrogen-containing compounds. Herein, we report our results on degradation and mineralization of DBT in aqueous solutions and in water-Triton X-100 at [Triton X-100] > CMC (critical micelle concentration) solutions using solar UV light and TiO₂ as a catalyst.

In general, the reaction kinetics follows the Langmuir-Hinshelwood mechanism given in the following equation:

$$r = \frac{kK[\text{DBT}]_0}{1 + K[\text{DBT}]_0} \quad (1)$$

where the reaction rate depends on the [DBT]₀, the equilibrium constant for DBT adsorption on the catalyst (TiO₂) and the rate constant of decomposition of the DBT-TiO₂ adduct, according to the following equation:



* Corresponding author. Tel.: +58 2129063317; fax: +58 2129063876.
E-mail address: onunez@usb.ve (O. Núñez).

In the last equation the difference between degradation and mineralization, from the kinetics point of view, is shown. In the first case, what is followed kinetically is the disappearance of DBT to form an intermediate. Meanwhile, the mineralization ($k_{\text{miner.}}$) consists of the formation of CO_2 , water and sulfate. The two rates are not necessarily equal since a stable intermediate may be formed making the mineralization slower than the degradation. It is important to remark that according to Eq. (1), the degradation reaction is not pseudo-first-order in [substrate]. However, plots of $\ln[\text{substrate}]$ vs. time give a good straight line which might be misinterpreted as a pseudo-first-order rate constant. We address this topic later in the paper.

When a second substrate, for instance Triton X-100, competes with DBT for the adsorption at the catalyst surface, Eq. (1) is transformed into the following equation:

$$r = \frac{kK[\text{DBT}]}{1 + K[\text{DBT}] + K'[\text{Triton X-100}]} \quad (3)$$

The rate of the competing Triton X-100 degradation is given by the following equation:

$$r = \frac{k'K'[\text{Triton X-100}]}{(1 + K[\text{DBT}] + K'[\text{Triton X-100}])} \quad (4)$$

In Eq. (4), K and k correspond to the adsorption equilibrium constant of the Triton X-100 on the TiO_2 catalyst and the rate constant of decomposition of the corresponding adduct. In this paper we show the feasibility of using Triton X-100 as a surfactant to improve the DBT solubility in water and its degradation under conditions in which the $[\text{Triton X-100}] > \text{CMC}$ (critical micelle concentration).

2. Materials and methods

2.1. Materials

The following reactants were used without further purification: dibenzothiophene, $\text{C}_{12}\text{H}_8\text{S}$, synthetic grade, Merck, dibenzothiophene 5,5 dioxide (sulfone), 98%, Merck, Triton X-100, $\text{C}_{34}\text{H}_{62}\text{O}_{11}$, 99.5%, Scharlau, Titanium dioxide (Anatase, P25), TiO_2 , 99.9%, Aldrich, phosphoric acid, H_3PO_4 , 87%, Riedel de Haen, potassium monobasic phosphoric acid, KH_2PO_4 , 99%, Riedel de Haen, potassium dibasic phosphoric acid, K_2HPO_4 , 98%, Riedel de Haen, hydrated potassium phosphate $\text{K}_3\text{PO}_4 \cdot \text{H}_2\text{O}$, 95%, Riedel de Haen, sodium hydroxide NaOH , 99%, Mallinckrodt, dichloromethane, Cl_2CH_2 , HPLC grade, Burdick & Jackson.

The following equipment was used: solar simulator, Solar Light Co. model LS 1000 UV fitted with a 1000 W xenon lamp to produce UV-B UV-A light at 290–400 nm; solar light radiometer, model PMA2100; millipore filtration equipment provided with cellulose and nitrocellulose 0.45 μm filters; diode arrangement UV-vis spectrophotometer, Hewlett Packard, model HP8452A; GCMS, Hewlett Packard model HP6890, mass detector: HP5973 and digital pH meter, model P211, Hanna Instruments.

2.2. Methods

2.2.1. UV DBT and DBT sulfone calibration curves

DBT solutions at pH 3, 7 and 10 (± 0.01) at 10 different concentrations in the range of 0.1–1.3 ppm at each pH were prepared using the corresponding phosphate buffer. Calibration curves were then constructed for the three pH values using the DBT absorption band at 232 nm. The following molar absorptivity (ϵ ($\text{Lcm}^{-1} \text{mol}^{-1}$)) was obtained at pH 3, 7 and 10, respectively: 8358 ± 334 , 9287 ± 371 and 7977 ± 319 .

DBT sulfone solutions at pH 7 at 10 different concentrations in the range 0.1–1.0 ppm were prepared using $\text{KH}_2\text{PO}_4/\text{K}_2\text{HPO}_4$ buffer in a ratio 1:10, sulfone: buffer. A DBT sulfone molar absorptivity (ϵ ($\text{Lcm}^{-1} \text{mol}^{-1}$)) of 44215 was obtained using one of the observed maximum absorption bands at 242 nm.

2.2.2. Photodegradation of solutions

In a 2 L beaker, 1 L of DBT solution was prepared using the required amount (0.3–1.3 mg) of DBT, TiO_2 (100 mg) and an amount of phosphate buffer (10 mg/L) to adjust the reaction pH to the desired one. This solution was magnetically stirred for 30 min. After this time, the beaker was placed under the solar simulator cannon (diameter ca. 20 cm) in such a way that the distance between the extremes of the cannon and the beaker was of 15 cm. The simulator was turned on. 3 mL solution aliquots were taken from the reactor at different times. These aliquots were filtered using millipore membranes and the UV spectrum of the filtered solution was recorded. The simulator radiation was measured using the radiometer. Typical radiation values of ca. 31 $\mu\text{W}/\text{cm}^2$ were used. The temperature of the reactor was kept constant at $22 \pm 1^\circ\text{C}$ by maintaining the temperature of the confined room where the simulator was located. The absorbance of each aliquot was transformed to concentration using the corresponding calibration curve. Plots of $\ln[\text{DBT}]$ vs. time were prepared in order to obtain the corresponding k_{obs} value. Using the initial concentration points and from the plot $[\text{DBT}]$ vs. time, the reaction rates were obtained.

The same procedure was used for the photodegradation of DBT sulfone 1 mg/L solution at pH 7.

2.2.3. DBT and DBT sulfone mineralization

DBT mineralization was followed by measuring the OCD (oxygen chemical demand) at pH 3, 7 and 10. In a typical sample a solution of 1.2 mg/L of DBT (1 L) with 100 mg of TiO_2 was irradiated using the solar simulator with a radiation intensity of ca. 31 $\mu\text{W}/\text{cm}^2$. The reaction temperature was kept constant at $22 \pm 1^\circ\text{C}$. Reaction aliquots (3 ml) were taken at different reaction times and the OCD in each aliquot was determined using the colorimetric method [17] in which the total organic sample content was oxidised using sulfuric acid and potassium dichromate for 2 h at 150°C . The solution absorbance at 600 nm was measured. From this absorbance, the solution OCD was obtained using a calibration curve made with potassium hydrogen phthalate.

The same procedure was used to follow the mineralization of the 1 mg/L solution of DBT sulfone at pH 7.

2.2.4. DBT degradation in Triton X-100 solutions

Solutions of DBT 10 mg/L, in Triton X-100 solutions (140–250 mg/L) were degraded at 22°C using TiO_2 and simulated solar light. DBT and Triton X-100 absorb light in the same UV region. However, it was found that the Triton X-100, at $[\text{Triton X-100}] > \text{CMC}$, does not suffer any degradation during the DBT degradation time (ca. 4 h). Therefore, the observed decrease in absorbance (A) corresponds to DBT degradation only. Therefore, from a plot of $\ln(A_t - A_{\text{inf}})$ vs. time, the degradation DBT rate constants in Triton X-100 solution were obtained.

2.2.5. Degradation reaction intermediates

Different DBT solutions (ca. 1.2 mg/L) were photodegraded at pH 7 using 100 mg of TiO_2 . The reaction was stopped at different times (40 and 90 min). The total reaction volume was filtered using millipore filters and the liquid was extracted with 90 mL of

dichloromethane. The extract was evaporated to a final volume of 1 mL. This sample was directly analyzed using GC/MS.

3. Results

3.1. DBT photodegradation

The kinetics of DBT solution degradation using disperse TiO_2 were determined by changing the initial DBT concentration at different solution pH 3, 7 and 10. At pH 7, changes in the amount of dispersed TiO_2 were also tested. It was found that in a plot of degradation % vs. mg of TiO_2 used (not shown) a plateau appeared at 100 mg/L of TiO_2 . Therefore, the latter amount of TiO_2 was used in all further experiments.

3.2. DBT degradation at different solution pH values

The solution decrease in DBT concentration was followed by UV–vis spectroscopy under acid, neutral and basic pH conditions. In Fig. 1, a typical absorbance vs. time degradation curve at pH 7 is shown. Similar curves were obtained at the other two pH studied (not shown).

A plot of [DBT] vs. time shows (Fig. 2) that, under conditions in which only light or only TiO_2 were used, no degradation was observed within 1 h. In Fig. 3, a plot of $\ln[\text{DBT}]$ vs. time is shown. As can be easily seen in the plot, the reaction became faster at acid pH. In Table 1, the apparent pseudo-first-order values obtained at the different [DBT] and pH conditions are shown. From the initial slope of a plot of [DBT] vs. time, the degradation velocities at each [DBT]₀ were obtained. The inverse of these values were plotted vs. $1/[\text{DBT}]_0$ and from the slope and intercepts of the curves the Langmuir–Hinshelwood k and K parameters were obtained at each pH. These values are shown in Table 2. In Fig. 4, plots of the rates at different [DBT]₀ at the three different pH values are shown. As can be seen, they are in good agreement with Eq. (1).

3.3. Identification of intermediates

Besides DBT, four intermediates were identified using GCMS at 40 and 90 min reaction times: benzaldehyde, benzoic acid, 2-cyclohexen-1-ol and 2-cyclohexene-1-one. The most intense signal corresponded to benzaldehyde.

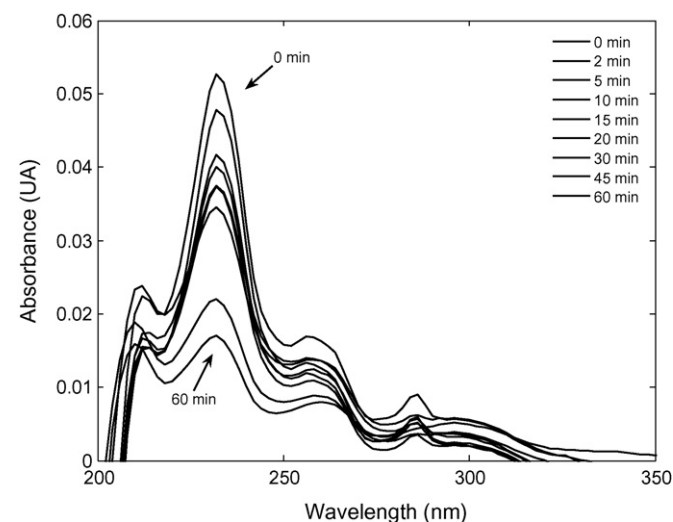


Fig. 1. Monitoring of the decrease in DBT absorbance at pH 7.00. [DBT]₀: 1.2 mg/L; radiation intensity: $31.20 \mu\text{W}/\text{cm}^2$; [TiO_2]: 100 mg/L.

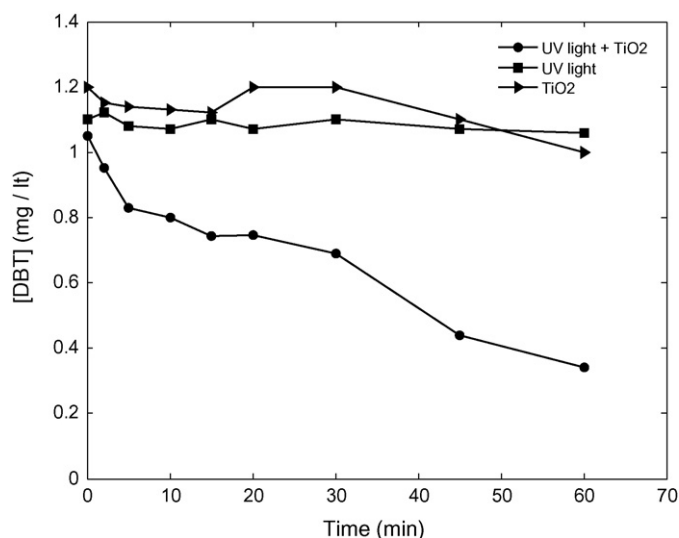


Fig. 2. Plot of [DBT] vs. time under different experimental conditions. [DBT]₀: 1.2 mg/L; radiation intensity: $31.20 \mu\text{W}/\text{cm}^2$; [TiO_2]: 100 mg/L; pH 7.00.

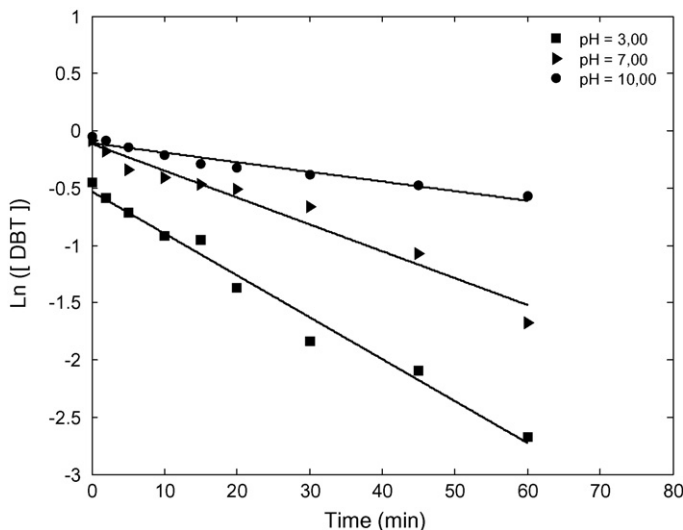


Fig. 3. Plot of $\ln[\text{DBT}]$ vs. time at the three solution pHs studied. [DBT]₀: 1.2 mg/L; radiation intensity: $32.79 \mu\text{W}/\text{cm}^2$; [TiO_2]: 100 mg/L.

Table 1

DBT degradation apparent pseudo-first-order rate constants (min^{-1}) and associated half time (min), obtained from the slope of the $\ln[\text{DBT}]$ vs. time plot

pH \pm 0.01	[DBT] (\pm 0.1 mg/L)	app. $k_{\text{obs}} \times 10^2$ (min^{-1})	$t_{1/2}$ (min)	R^2
3.00	0.40	5.82 ± 0.11	12 ± 1	0.997
	0.60	4.45 ± 0.03	16 ± 1	0.999
	0.80	3.96 ± 0.10	18 ± 1	0.994
	1.00	3.66 ± 0.17	19 ± 1	0.981
	1.20	2.96 ± 0.18	23 ± 2	0.965
7.00	0.40	4.91 ± 0.41	14 ± 1	0.936
	0.60	2.76 ± 0.20	25 ± 2	0.950
	0.80	2.36 ± 0.12	29 ± 2	0.976
	1.00	2.35 ± 0.16	30 ± 2	0.959
	1.20	1.71 ± 0.12	40 ± 3	0.958
10.00	0.40	0.912 ± 0.072	76 ± 6	0.944
	0.60	0.881 ± 0.065	79 ± 6	0.949
	0.80	0.953 ± 0.072	73 ± 6	0.946
	1.00	0.839 ± 0.061	83 ± 6	0.950
	1.20	0.740 ± 0.062	94 ± 8	0.933

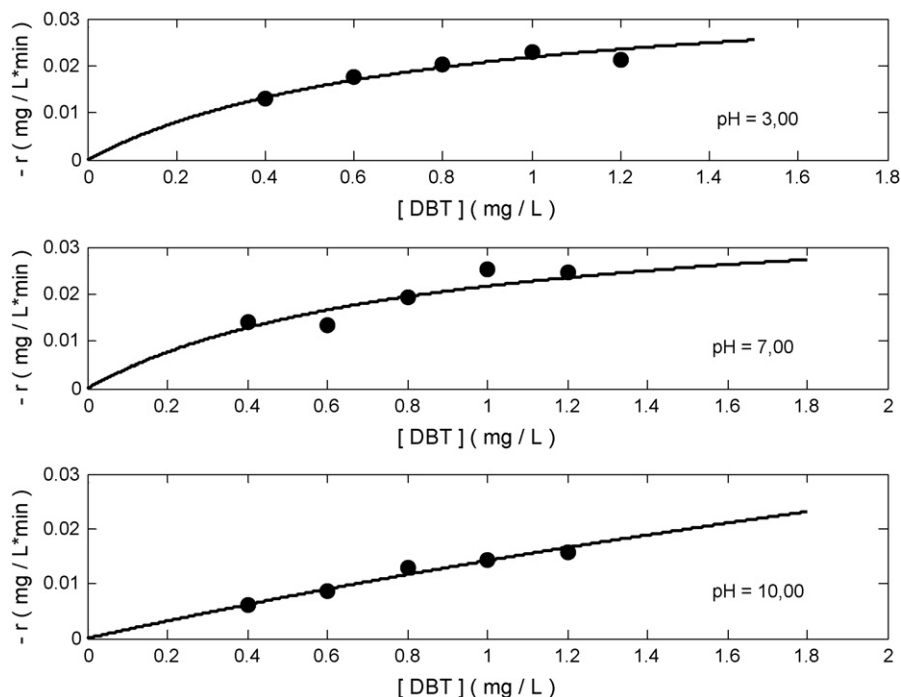


Fig. 4. Plots of rates vs. $[DBT]_0$ at the three reaction pHs studied in this work.

Table 2
DBT Langmuir–Hinshelwood parameters at the studied pH values

pH \pm 0.01	K (L mg ⁻¹)	k (mg L ⁻¹ min ⁻¹)	kK (min ⁻¹)
3.00	1.3143 \pm 0.3256	0.0384 \pm 0.0068	0.0505 \pm 0.0075
7.00	1.1629 \pm 0.3971	0.0403 \pm 0.0092	0.0468 \pm 0.0079
10.00	0.1518 \pm 0.0436	0.1075 \pm 0.0088	0.0163 \pm 0.0013

3.4. DBT mineralization

In Fig. 5 plots of $\ln(OCD)$ vs. time at pH 3, 7 and 10, are shown. From the slope of these straight lines the apparent pseudo-first-order rate constants for DBT mineralization are obtained. These rate constants are shown in Table 3 where they are compared with the corresponding rate constants for DBT degradation.

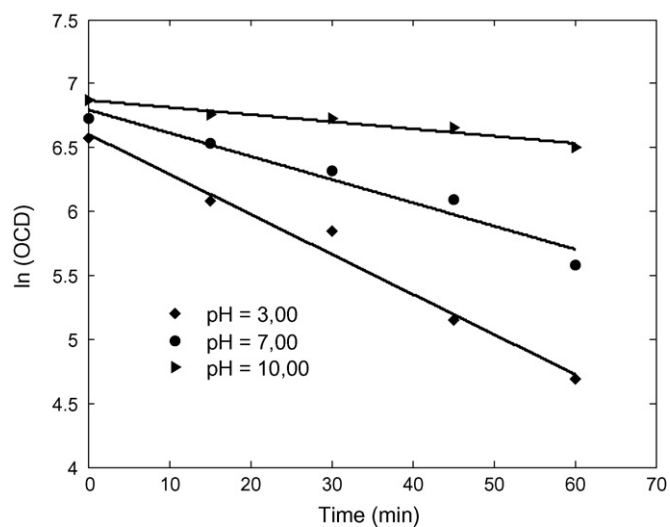


Fig. 5. DBT mineralization. Plot of $\ln(OCD)$ vs. time at the three different pH values studied.

3.5. Degradation and mineralization of DBT 5,5 dioxide (sulfone)

In Fig. 6 degradation of DBT and its corresponding sulfone (DBT 5,5 dioxide) at pH 7 and 22 °C \pm 1 are shown. The rate constants obtained from the straight lines slopes are reported in

Table 3
Comparison between the rate constants obtained for mineralization and degradation of DBT at pH 3, 7 and 10

pH \pm 0.01	$k_{\text{osb}} \times 10^2$ (min ⁻¹), mineralization (k_{miner})	$k_{\text{osb}} \times 10^2$ (min ⁻¹), degradation (k_{deg})
3.00	3.13 \pm 0.23	2.96 \pm 0.18
7.00	1.82 \pm 0.27 (8.43) ^a	1.71 \pm 0.12 (8.65) ^b
10.00	0.561 \pm 0.096	0.740 \pm 0.062

^a The value in parentheses corresponds to de DBT 5,5 dioxide (sulfone) mineralization rate.

^b The value in parentheses corresponds to the DBT 5,5 dioxide (sulfone) degradation rate (Fig. 6).

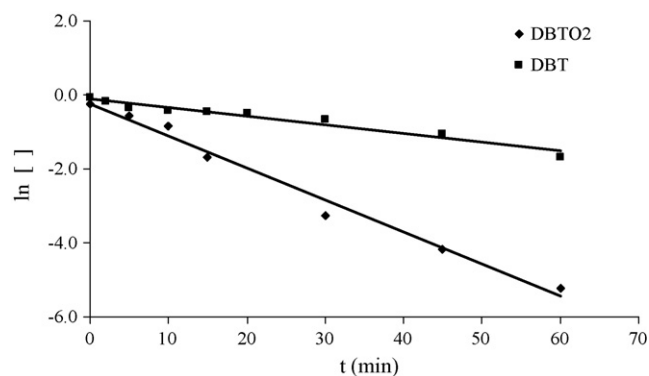


Fig. 6. DBT dioxide (sulfone) and DBT degradation. From the slope rate constants of 0.086 and 0.023 min⁻¹ are obtained for the sulfone (DBTO2) and DBT, respectively. Reaction conditions: initial reactant concentration: 1 mg/L; pH 7; $[TiO_2] = 100$ mg/L; $T = 22$ °C \pm 1; radiation intensity: 32.79 μ W/cm².

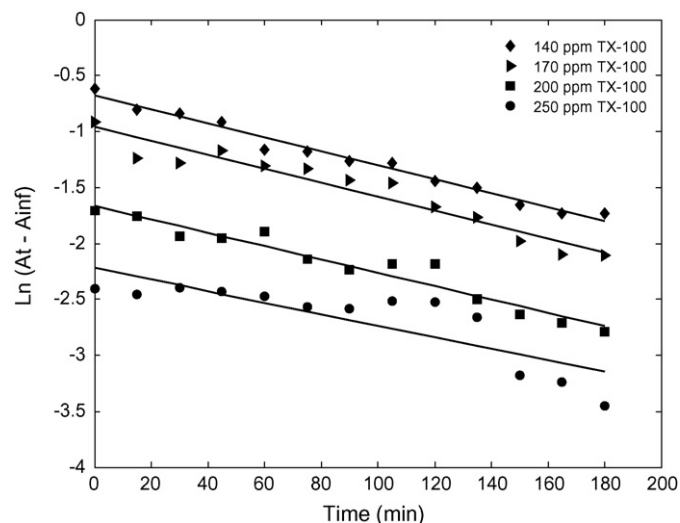


Fig. 7. Plot of $\ln(A_t - A_{inf})$ vs. time for DBT in Triton X-100 solutions. [DBT]: 10 mg/L; average radiation intensity: $27.64 \mu\text{W}/\text{cm}^2$; pH: 7.00. A_t : absorbance at time t ; A_{inf} : absorbance at time infinite.

Table 4

Apparent pseudo-first-order rate constants for DBT degradation in Triton X-100 solutions where $[\text{Triton X-100}] > \text{CMC}$

[Triton X-100] (± 1 mg/L)	$k_{obs} \times 10^3$ (min^{-1})	R^2
140	6.40 ± 0.21	0.981
170	6.21 ± 0.42	0.923
200	5.95 ± 0.36	0.941
250	5.15 ± 0.80	0.748

pH 7.

Table 3. In this table the sulfone mineralization rate constant is also reported.

3.6. Degradation of DBT in Triton X-100 solutions

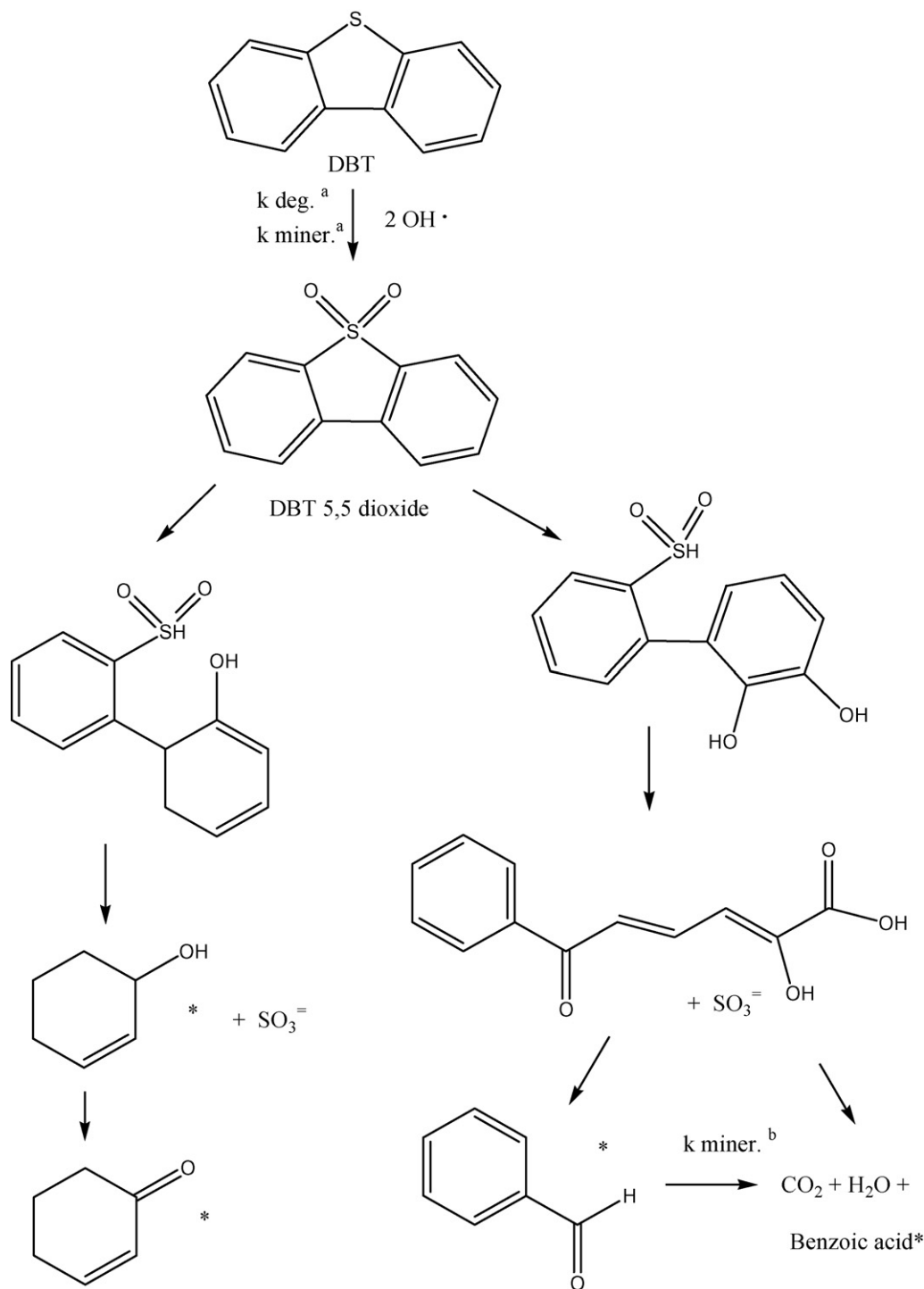
The extent of Triton X-100 degradation, under the conditions $[\text{Triton X-100}] > \text{CMC}$, was studied in order to explore its feasibility to improve DBT solubility and degradation. From plots of $[\text{Triton X-100}]_0$ vs. time it is observed that there is no Triton X-100 degradation during 2 h reaction time. In Fig. 7, DBT degradation, under conditions: $[\text{Triton X-100}] > \text{CMC}$ and $[\text{DBT}] = 10$ ppm, are also shown. In Table 4, the pseudo-first-order rate constants for DBT degradation in Triton X-100 solution ($[\text{Triton X-100}] > \text{CMC}$) obtained from the slope of the straight lines of Fig. 7 are shown.

4. Discussion

4.1. DBT degradation in water solutions

As shown in Fig. 1, DBT readily decomposed ($t_{1/2}$ ca. 30 min, at pH 7) when treated with disperse TiO_2 and UV simulated solar light. The kinetics of the reaction can be followed conveniently by monitoring the DBT absorption band at 232 nm. The observed catalysis is due to the combined effect of UV irradiation and TiO_2 as a catalyst. This fact is supported by the results (Fig. 2) where experiments with simulated UV solar light and TiO_2 are compared with the ones with only light or only TiO_2 . This observation is important to note since an important degradation contribution coming only from photocatalysis and mass transport from the water to air is frequently found. Following the DBT degradation at 232 nm it was possible then to obtain straight lines from plots of $\ln[\text{DBT}]$ vs. time

at different pH. These plots are shown in Fig. 3. It is straightforward to conclude, by comparing the slopes of these lines, that the reaction at pH 3 is the fastest. According to the Langmuir–Hinshelwood model, two parameters determine the reaction rate (Eq. (1)): the absorption equilibrium constant (K) and the DBT– TiO_2 adduct decomposition rate constant (k). In fact, k corresponds to an apparent rate constant with units of M time^{-1} , but $k \times K$ corresponds to a pseudo-first-order rate constant with units of time^{-1} . Hence, the experimentally determined pseudo-first-order rate constants (k_{obs}), for instance those obtained from the slopes of the straight lines of Fig. 3, should match the $k \times K$ values obtained from plots of $1/\text{rate}$ vs. $1/[\text{DBT}]_0$. Furthermore, according to Eq. (1), $k \times K$ is equal to k_{obs} only when $1 \gg K[\text{DBT}]_0$; otherwise, $k_{obs} = kK/(1 + K[\text{DBT}]_0)$ and it is not a pseudo-first-order rate constant even though an apparent straight line could be obtained. For instance, see the r^2 values in Table 1 for the apparent straight lines obtained at pH 3, 7 and 10. In fact, from this table it is clear that the reported rate constants are not pseudo-first-order rate constants at all since they change with the $[\text{DBT}]_0$. In Table 2, the k , K and $k \times K$ obtained from plots of $1/\text{rate}$ vs. $1/[\text{DBT}]_0$ are shown. As can be seen from the table, the $k \times K$ values are of the same order of magnitude, but not equal, to the k_{obs} values reported in Table 1. Therefore we talk about apparent k_{obs} values instead of k_{obs} values. It could also be proved that the decrease in the k_{obs} values with increasing $[\text{DBT}]_0$ is due to the light as limiting reagent. However, if this were the case, at higher $[\text{DBT}]_0$ a levelling in the k_{obs} values should be obtained. On the contrary the levelling is observed at low $[\text{DBT}]_0$, when $K[\text{DBT}] < 1$ as predicted by Eq. (1) in which the rate vs. $[\text{DBT}]_0$ profile becomes a straight line at low $K[\text{DBT}]_0$ value. In fact, in Fig. 4 a direct plot of the initial rate values vs. time, for the three pH studied in this work, are shown. From these plots it can be concluded that, in fact, for the three pH the Langmuir–Hinshelwood mechanism is operating since the experimental points can be fit to Eq. (1). Only in the case of pH 10, the rate vs. time plot approaches a straight line. This indicates, that only in this case, $1 \gg K[\text{DBT}]_0$ and $\text{rate} = k \times K [\text{DBT}]_0$; that is, a first order reaction rate where $k_{obs} = k \times K$. At the other two pH values, $\text{rate} = k \times K[\text{DBT}]_0/(1 + K[\text{DBT}]_0)$ and $k_{obs} = k \times K/(1 + K[\text{DBT}]_0)$. Therefore, at high pH the K term is unfavourable since $K[\text{DBT}]_0 < 1$ (see K values in Table 2). On the contrary, the K value at pH 3 is such that $K[\text{DBT}]_0 > 1$. From this table, it can be concluded that the degradation of DBT is more efficient at pH 3, since the favourable K values more than balance the unfavourable k values, decreasing with decreasing pH. The K value is more favourable at acid pH due to the positive charged TiO_2 surface (pH of zero charge ca. 6.5 [18]) that interacts better for instance, with free electrons on sulfur. The fact that the rate constant k increases with pH evidences that the decomposition occurs via radicals since at higher pH there will be more OH^\bullet , thus accelerating the DBT degradation. The radical participation is reinforced by the reported [19] photodegradation of DBT in acetonitrile in which DBT degradation occurs ca. 40 times slower ($t_{1/2} = 19.8$ h) than the degradation reported in this work ($t_{1/2}$ ca. 30 min) for instance at pH 7. From GC/MS degradation fractions, spectra (not shown) taken at 40 and 90 min, benzaldehyde was detected as main component. There were also detected three minor compounds: benzoic acid, 2-cyclohexen-1-ol and 2-cyclohexene-1-one. In Scheme 1, a degradation scheme is proposed. This proposal is in agreement with the metabolic DBT desulfuration scheme suggested by Van Afferden et al. [20]. As shown in Table 3, the rate constants for degradation and mineralization (following OCD) are the same (within the experimental error) at neutral and acid pH. However, at pH 10, the mineralization is 25% slower than the DBT degradation. Therefore, at neutral and acid pH, the photocatalysis rate limiting step is the same for degradation and mineralization. However, at basic pH, the rate limiting step for mineralization is not the same as that for degradation. Probably, benzaldehyde decom-

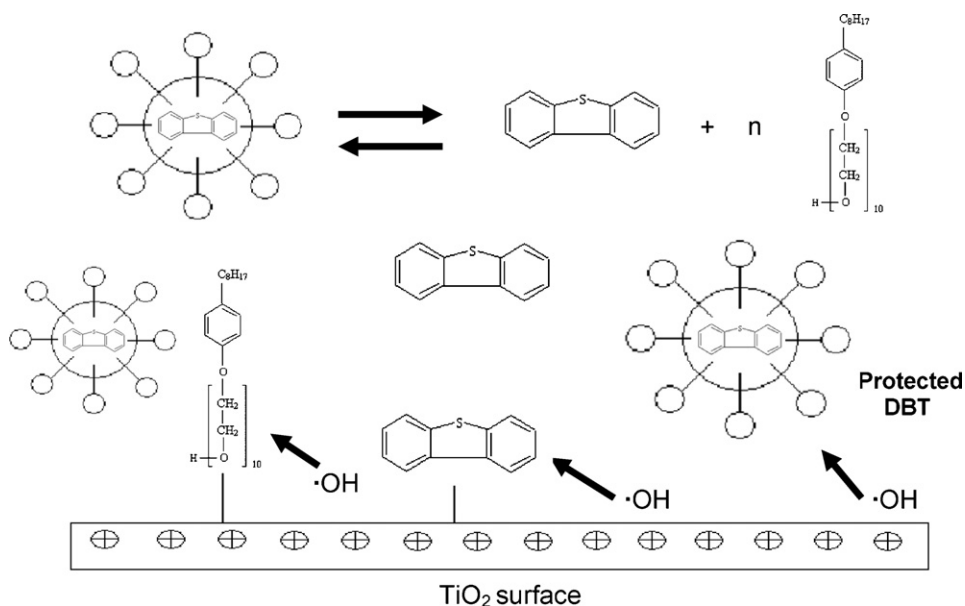


Scheme 1. Possible DBT photocatalyzed degradation path. Compounds marked with *, correspond to intermediates detected by GC/MS. a: corresponds to the confirmed rate limiting steps for degradation and mineralization at pH 7. b: possible rate limiting step for mineralization at pH 10.

position becomes the rate limiting step for the mineralization (see Scheme 1). The obtained degradation rate ($k_{\text{deg.}} = 0.086 \text{ min}^{-1}$) for DBT sulfone (Fig. 6 and Table 3) is ca. four times faster than the DBT degradation rate. This result confirms Scheme 1 proposal of DBT sulfone formation as the rate limiting for DBT degradation. The DBT sulfone mineralization rate ($k_{\text{miner.}} = 0.084 \text{ min}^{-1}$, Table 3) is the same as the one obtained for its degradation at pH 7. This result also confirms that DBT degradation and mineralization have the same rate limiting (DBT sulfone formation) at pH 7.

4.2. DBT degradation in Triton X-100 water solutions

Triton X-100 solutions at $[\text{Triton X-100}] > \text{CMC}$ dissolve DBT to concentrations one-order of magnitude higher than its solubility in water. In fact, DBT solutions of 10 mg/L were prepared using Triton X-100 solutions. The main goal in using Triton X-100 was to increase the DBT solubility without affecting its degradation/mineralization rates. A good sign that this goal can be accomplished is that no degradation of Triton X-100, at $[\text{Triton X-100}] > \text{CMC}$, is observed



Scheme 2. TiO_2 surface interaction with DBT and Triton X-100 monomers. DBT in Triton X-100 micelles is protected from degradation. Only Triton X-100 in solution competes with DBT.

in reaction periods of ca. 2 h. Therefore, no competition with DBT degradation is expected in mixtures of DBT with Triton X-100. However, at longer reaction times, some competition may affect the DBT degradation according to Eq. (3) if the term $K' \times [\text{Triton X-100}]$ becomes important. In fact, as shown in Fig. 7, the DBT degradation rate constants (slope of the lines) decrease with increasing [Triton X-100]. However, there is a smooth change in slope as seen in Table 4. As shown in Scheme 2, Triton X-100 in its micelle form acts as a DBT reservoir in equilibrium with DBT in solution i.e. the form that reacts at the TiO_2 surface. The micelle form of Triton X-100 does not react at the TiO_2 surface, probably due to steric effects. However, Triton X-100 monomers can react at the catalyst surface competing with DBT for the active site. Therefore, as the experimental results show, when the [Triton X-100] is increased there is a decrease in the DBT degradation rate, as expected according to Eq. (3), since there is higher free monomer concentration. When the degradation rate constants shown in Table 4 are compared with the ones at pH 7 at Table 1, a retardation of one-order of magnitude is found in the Triton X-100 solutions DBT degradation. However, it is important to point out that in the latter case a 10 mg/L DBT solution is degraded. Meanwhile, under Table 1 conditions only 1.2 mg/L of DBT can be dissolved due to the DBT saturation concentration in water. This result demonstrate that the use of TiO_2 /solar light technology may be useful for the treatment, for instance, of rich-sulphur asphaltene (heavy oil) contaminated solids via washing the solid with Triton X-100 solution and treating the liquid with this technology.

5. Conclusions

DBT in aqueous solution (1.2 mg/L) readily decomposes ($t_{1/2}$ ca. 20 min at pH 3 and 30 min at pH 7) when treated with solar light and disperse anatase TiO_2 (100 mg/L). DBT decomposition occurs according to the Langmuir–Hinshelwood mechanism. Only for decomposition at pH 10, $k_{\text{obs}} = k \times K$, that is, a pseudo-first-order rate constant. In the other cases, $k_{\text{obs}} = k \times K/(1 + K[\text{DBT}])$. Therefore, an apparent k_{obs} depends inversely on the $[\text{DBT}]_0$. The fastest rate is obtained at pH 3 due to a favourable DBT adsorption on the TiO_2 positive charged surface that more than balances the rather small value for the DBT-adduct decomposition that is catalyzed by the presence of OH radicals. The rates of DBT mineralization are quite

similar to the degradation rates, except at pH 10 where $k_{\text{miner.}} < k_{\text{deg.}}$. Therefore, at neutral and acid pH, the mineralization rate limiting step is the same as the degradation one. This rate limiting step correspond to the DBT sulfone formation as has been found [5,12,21] with other oxidants.

Conditions to degrade/mineralize ($t_{1/2}$ ca. 110 min) up to 10 mg/L DBT water solutions were found using Triton X-100 surfactant at [Triton X-100] > CMC. The Triton X-100 micelle acts as a DBT reservoir in equilibrium with the DBT in solution. The Triton X-100 monomers compete with the DBT for the TiO_2 active site. Therefore, faster rates are obtained at [DBT] close to the CMC.

Acknowledgements

We acknowledge the Environment Management Unit (UGA) at Simon Bolivar University for financial support. We also grateful to the Royal College of Surgeons in Ireland and in particular Prof. Kevin Nolan for his hospitality and support during the sabbatical of one of the authors (ON) during which part of this manuscript was written. We also acknowledge Lucianna Viele for her technical support.

References

- [1] I.V. Babich, J.A. Moulijn, Fuel 82 (6) (2003) 607–631.
- [2] T. Aida, D. Yamamoto, Preprints. Pap.-Am. Chem. Soc., Div. Fuel Chem. 39 (2) (1994) 623–626.
- [3] X. Ma, K. Sakanishi, I. Mochida, Ind. Eng. Chem. Res. 33 (2) (1994) 218–222.
- [4] D.D. Whitehurst, T. Isoda, I. Mochida, Adv. Catal. 42 (1998) 345–471.
- [5] R.B. LaCount, S. Friedman, J. Org. Chem. 42 (16) (1977) 2751–2754.
- [6] P. De Filippis, M. Scarsella, Energy Fuels 17 (2003) 1452–1455.
- [7] S.E. Bonde, W. Gore, G.E. Dolbear, E.R. Skov, Preprints. Pap. Am. Chem. Soc., Div. Pet. Chem. 45 (2) (2000) 364–366.
- [8] P.S. Tam, J.R. Kittrell, J.W. Eldridge, Ind. Eng. Chem. Res. 29 (3) (1990) 321–324.
- [9] J.H. Baxendale, M.G. Evans, G.S. Park, Trans. Faraday Soc. 42 (1946) 155–169.
- [10] K. Kirimura, T. Furuya, Y. Nishii, Y. Ishii, K. Kino, S. Usami, J. Biosci. Bioeng. 91 (3) (2001) 262–266.
- [11] J.J. Garcia, P.M. Maitlis, J. Am. Chem. Soc. 115 (1993) 12200–12201.
- [12] K. Yasu, Y. Yamamoto, T. Furuya, K. Miki, K. Ukegawa, Energy Fuels 15 (6) (2001) 1535–1536.
- [13] M. Alvaro, E. Carbonell, H. García, Appl. Catal. B: Environ. 51 (3) (2004) 195–202.
- [14] A. Núñez, G. Pardo, O. Núñez, Oil Industry Liquid Waste Treatment: Our Laboratory Experience. Química Sustentable en Universidades Latinoamericanas, Universidad Nacional del Litoral (UNL), Argentina, 2003.

- [15] N. Barrios, P. Sivov, D. D'Andrea, O. Núñez, *Int. J. Chem. Kinet.* 37 (7) (2005) 414–419.
- [16] I. Kuehr, O. Núñez, *Pest Manage. Sci.* 63 (5) (2007) 491–494.
- [17] W. Boyles, *The Science of Chemical Oxygen Demand*, Technical Information Series, Booklet No. 9, Hach Company, USA, 1997.
- [18] J. Zhao, K. Wu, T. Wu, H. Hidaka, N. Serpone, *J. Chem. Soc., Faraday Trans.* 94 (5) (1998) 673–676.
- [19] S. Matsuzawa, J. Tanaka, S. Sato, T. Ibusuki, *J. Photochem. Photobiol. A* 149 (2002) 183–189.
- [20] M. Van Afferden, S. Schacht, J. Klein, H. Trueper, *Arch. Microbiol.* 153 (4) (1990) 324–328.
- [21] S. Murata, K. Murata, K. Kidena, M. Nomura, *Energy Fuels* 18 (1) (2004) 116–121.